Available online at www.sciencedirect.com
SCIENCE DIRECT®
European Journal of Medicinal Chemistry 40 (2005) 1316–1324
EUROPEAN JOURNAL OF MEDICINAL CHEMISTRY
www.elsevier.com/locate/ejmech

Original article

A new potential cyclooxygenase-2 inhibitor, pyridinic analogue of nimesulide

Catherine Michaux [a,*], Caroline Charlier [a], Fabien Julémont [b], Xavier de Leval [b], Jean-Michel Dogné [b], Bernard Pirotte [b], François Durant [a]

[a] *Laboratoire Chimie Biologique Structurale, Facultés Universitaires N.-D. de la Paix, 61, rue de Bruxelles, B-5000 Namur, Belgium*
[b] *Laboratoire de Chimie Pharmaceutique, Centre interfacultaire de recherche en pharmacochimie des substances naturelles et synthétiques, Université de Liège (Ulg), 1, avenue de l'hôpital, B-4000 Liège, Belgium*

Received 2 December 2004; received in revised form 14 August 2005; accepted 25 August 2005

Available online 11 October 2005

Abstract

In this paper, the binding mode of original pyridinic compounds structurally related to nimesulide, a preferential cyclooxygenase (COX)-2 inhibitor, is analyzed by docking simulations in order to understand structure–activity relationships of this family. Structural modifications are proposed to reverse the selectivity of the more active inhibitor of the series characterized by a preferential activity on COX-1. On the basis of these modifications, a new compound with a bromo substituent was designed and showed a COX-2 selective inhibition.

Keywords: COX-2 selective inhibitor; Molecular modeling studies; Pyridinic compounds; Interactions model

1. Introduction

Non-steroidal anti-inflammatory drugs (NSAIDs) are widely used for the treatment of rheumatism diseases, as rheumatoid arthritis, and pain [1]. The pharmacological effects of NSAIDs are due to inhibition of a membrane enzyme called cyclooxygenase (COX) which is involved in the prostaglandin biosynthesis [2]. The discovery in 1990 of two isoforms, COX-1 and COX-2, helped to understand the side-effects of NSAIDs [3]. The constitutive COX-1 is found in healthy populations and has mainly a physiological role in kidneys and the stomach. In contrast, the mainly inducible COX-2 is involved in the production of prostaglandins mediating pain and supporting the inflammatory process [4,5].

Classical NSAIDs such as aspirin and ibuprofen non-selectively inhibit both isoenzymes and cause gastric failure like bleeding and ulcer [6,7]. In order to prevent or decrease these side-effects, a current strategy consists of designing selective COX-2 inhibitors as NSAIDs with an improved gastric safety profile [8,9].

Recent data show that the biological functions of prostanoids, mediators formed by the two enzymes, are much more complex and interrelated than previously appreciated [10]. Experimental evidence indicates that a full inflammatory response is likely sustained by prostanoids generated by both enzymes. Similarly, inhibition of both isoforms is necessary for gastrointestinal mucosal damage to develop and both enzymes contribute to normal renal function. Moreover, the synthesis of endothelial prostacyclin is mainly driven by COX-2, so that the selective COX-2 inhibition may bias vascular prostaglandin synthesis in favor of COX-1-derived thromboxane A_2 in platelets. This could explain the cardiotoxicity of the rofecoxib (Vioxx®), which was withdrawn in September 2004 [11].

Therefore, it is not obvious whether a high level of COX-2 selectivity confers any advantages. On the contrary, the design of COX-2 "preferential" inhibitors keeping a slight effect on COX-1 at therapeutic dosage could theoretically limit the imbalance prostacyclin/thromboxane A_2 leading to cardiovascular side-effects. The question of the efficacy and the limitations of gastrointestinal side-effects with these preferential inhibitors should be further evaluated.

Moreover, a third variant of the COX enzyme, COX-3, recently identified in the brain, was found to be composed of

* Corresponding author. Tel.: +32 81 72 4555; fax: +32 81 72 4530.
E-mail address: catherine.michaux@fundp.ac.be (C. Michaux).

0223-5234/$ - see front matter © 2005 Elsevier SAS. All rights reserved.
doi:10.1016/j.ejmech.2005.08.003

COX-1 and the retained intron 1 [12–14]. It was considered at first as a potential target of paracetamol, but it was later found that COX-3 inhibition by paracetamol is not specific and rather weak, and therefore cannot account completely for its inherent discrepancies. Anyway, identification of this isoenzyme will open a new chapter in anti-inflammatory and analgesic agents. However, a frame shift caused by complete retention of intron 1 in the human sequence questions its relevance to human pathophysiology. In addition, only canine COX-3 would possess COX activity.

Nevertheless, it is still interesting to perform research on new COX-2 compounds and try to design original structurally families of COX-2 inhibitors with an appropriate balance between COX-1 and COX-2 inhibition. Such new agents could also play a positive role in other pathophysiological processes involving COX-2, and particularly in cancerogenesis and neurodegenerative disorders such as Alzheimer's and Parkinson's diseases [15–17].

Nimesulide (**1**) is one of the first NSAIDs marketed, with a preferential COX-2 inhibition profile [18–20]. Several original pyridinic compounds derived from this drug were synthesized and their COX inhibitory effects evaluated with a whole blood assay (Fig. 1) [21]. On the basis of physicochemical studies (pK_a determination by spectrophotometry) and structural analyses (^{1}H-NMR, IR and X-ray diffraction) previously reported in [21], it was assumed that **1**–**4** showed different ionic states at physiological pH (Fig. 2). The sulfonamide group is mainly deprotonated in **1**–**3** and a pyridinium moiety is found in **3**. Compound **4** is mainly non-

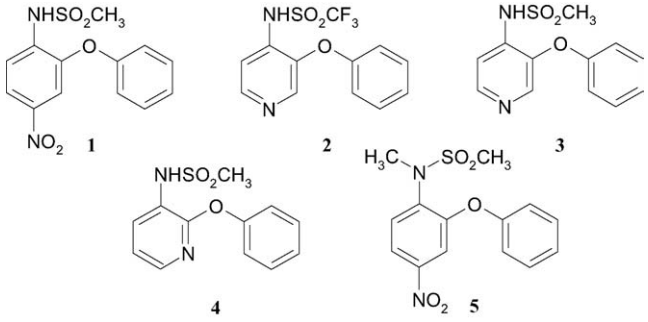

Fig. 1. Structure of nimesulide (**1**) and its analogues (**2**–**5**).

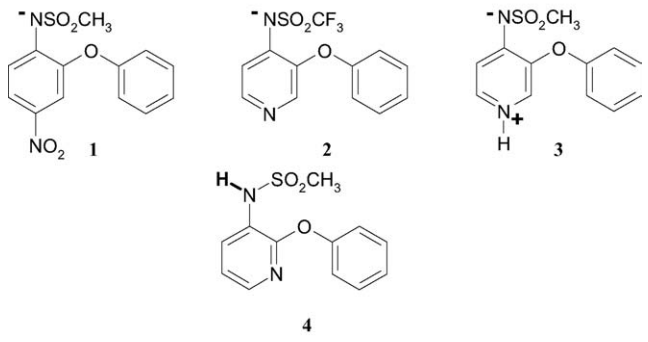

Fig. 2. Major ionic state at physiological pH of nimesulide and its analogues **1**–**4**, determined by physicochemical studies (pK_a determination by spectrophotometry) and structural analyses (^{1}H-NMR, IR and X-ray diffraction).

ionized at pH 7.4. These major forms are supposed to interact with the COX enzymes.

In this contribution, COX-1 and COX-2 inhibitory potency of derivatives of nimesulide was first evaluated in an enzymatic assay. Indeed, unlike the whole blood assay, such test reflects the best the pure ligand–enzyme interactions. Secondly, their in vitro activities were rationalized and their potential binding modes in human COXs explored by docking studies. On the basis of these analyses, structural modifications were investigated to enhance activity and selectivity of this series of compounds. A new COX-2 selective lead compound was then identified.

2. Method

2.1. Chemistry

The chemistry of the compounds presented in this publication was described elsewhere [21,22].

2.2. Biological assay

Depending on the assay used to determine COX inhibitory activity, results can vary. In this study, in vitro enzymatic assays were used as they are more directly explained by docking studies. As human COX-1 is not commercially available, the in vitro COX inhibitory assay was determined by using purified ovine COX enzymes. In this way, comparison of both isoforms is valid and gives idea of the selectivity of the new compounds. For technical reasons, two different ovine COXs assays were used and a human COX-2 assay was also performed.

The enzymes were purchased from Cayman Chemical Company. The human recombinant COX-2 was isolated from a baculovirus overexpression system in Sf21 cells. Its purity is approximately 70%. The ovine COX-1 and COX-2 enzymes were isolated from ram seminal vesicles and from sheep placenta, respectively. The purity is 95% and 70%, respectively.

The inhibitory potency was assayed **a)** with purified ovine enzyme [23]; **b)** with human purified COX-2 enzyme in the same way as in assay **a** but with ligand–enzyme incubation time of 5 min and with arachidonic acid incubation time of 3 min or; **c)** with a COX (ovine) inhibitor screening kit (catalog no. 560101, Cayman Chemical, Ann Arbor, MI). All the values are averages over three experiments. Table 1 summarizes the parameters for each assay performed. The human COX-2 assay was not performed following assay **a**, because the optimal conditions for the human COX-2 activity are not strictly the same as for the ovine one.

In general, the COX inhibitory activity was determined by measuring non-enzymatically PGE_2 or $PGF_{2\alpha}$ (by $SnCl_2$ reduction of COX-derived PGH_2) production from arachidonic acid, substrate of COX enzymes. The COX enzymes (1 unit: consumes 1 O_2 nanomol per min at 37 °C in 0.1 M Tris–HCl pH 8, 2×10^{-3} M phenol, 1×10^{-6} M hematin and

Table 1
Characteristics of the performed assays

Assay	Isoforms	Incubation time of drug with enzyme (min)	Incubation time with AA (min) at 37 °C	Final [AA] (μmol l^{-1})	End of the reaction	Measure of the activity
a)	Ovine COX-1 and COX-2	60 at 0 °C	2	10	Addition of diclofenac sodium salt (1 mM) at 0 °C	PGE_2 production quantified by RIA
b)	Human COX-2	5 at 37 °C	3	10	Addition of diclofenac sodium salt (1 mM) at 0 °C	PGE_2 production quantified by RIA
c)	Ovine COX-1 and COX-2	5 at 37 °C	2	100	Addition of HCl (1 M) at 0 °C	$PGF_{2\alpha}$ production quantified by EIA

1×10^{-4} M arachidonic acid) were first incubated with drugs (diluted in 0.2–1% DMSO) in their optimal activity conditions: pH 8, 37 °C and with two cofactors (hematin and phenol). Then sodium arachidonate was added and incubation is continued. After the enzymatic reaction was stopped, PGE_2 or $PGF_{2\alpha}$ production was measured by radio- or enzyme immunoassay.

2.3. Docking studies

Homology modeling of the human isoforms was performed using *Homology* from the *InsightII* package [24].

Research performs exploration of one region of the protein (rigid) by one ligand (flexible) [25]. The hypothesis generation is based on a Monte Carlo algorithm, randomly generating conformations. Cutoff: 15 Å; Ecut: –10 kcal mol^{-1}; ntrials: 10,000.

Gold is a genetic algorithm for docking flexible ligands into protein binding sites [26]. Conformation of some amino acids (Ser, Thr and Lys) is optimized during the run. Popsiz = 100; maxops = 100,000; niche_size = 2.

Autodock uses a hybrid method called Lamarckian Genetic Algorithm (genetic algorithm coupled with a local search) to predict the interaction of ligands with macromolecular targets [27]. Runs: 200; population size: 50; number of generations: 27,000.

Discover3 uses the molecular mechanics to optimize the conformation of the ligand–protein complexes and evaluate the interaction energy (ΔEvdw and ΔEcb) [28]. The backbone is moved following force constants and side-chains move freely.

Forcefield: ESFF; dielectric constant: 1*r; criteria convergence: 10 kcal mol^{-1} for the Steepest Descent algorithm, 0.01 for the Conjugate Gradient one.

Delphi provides numerical solutions to the Poisson–Boltzmann equation for molecules of arbitrary shape and charge distribution [29]. It allows calculation of the electrostatic contribution to the solvation energy of a molecule (ΔEsolv).

Molecular electrostatic potential (*MEP*) profiles were calculated from the optimized structure of each moiety using quantum mechanics, with HF method and 6-31G* basis set [30].

3. Results and discussion

3.1. Enzymatic assay of the COX inhibitory effect

Ability of compounds **1–5** to inhibit COX-1 and -2 was evaluated using enzymatic assays **a** and **b** (Table 2). NS-398 and indomethacin, a COX-2 selective and a non-selective inhibitor, respectively, were also tested as references. Although IC_{50} of **1** is above 100 μM for the two isoforms, it preferentially inhibits COX-2 at 100, 10 and 1 μM. Compounds **3–5** are considered to be inactive or not very active. Compound **2** exhibits an inhibitory activity on both COXs with a preferential effect on COX-1, unlike **1**. Compound **2** was therefore selected for further analyses.

COX-2 IC_{50} values for **1** are markedly higher than values found in literature. However, the selectivity ratio estimated by different research groups, albeit in the same test, can be

Table 2
Estimated IC_{50} values and % inhibition on enzymatic assay **a** and **b** for **1–5**, NS-398 and indomethacin

Compound	IC_{50} COX-1 ovine*,a (μM)	% Inhibition ovine COX-1*,a (100 μM)	IC_{50} COX-2 ovine*, a/human*,b (μM)	% Inhibition ovine COX-2*,a (100 μM)
1	> 100	–1.62 ± 4.10	> 100/97.5	34.79 ± 3.54
2	3.66	93.77 ± 5.68	82.7/ > 100	57.56 ± 10.68
3	> 100	0.72 ± 5.27	> 100	–1.87 ± 1.05
4	> 100	2.41 ± 0.93	> 100	4.24 ± 1.98
5	> 100	14.88 ± 4.80	> 100	19.35 ± 6.68
NS-398	> 100	20.06 ± 5.39	57.1/0.5	52.64 ± 2.36
Indomethacin	0.1	92.68 ± 1.67	0.5/0.4	81.91 ± 2.08

* Details in experimental section.
[a] Assay **a**: enzyme–ligand incubation time of 1 h and arachidonic acid incubation time of 2 min.
[b] Assay **b**: enzyme–ligand incubation time of 5 min and arachidonic acid incubation time of 3 min.

quite different. Therefore, it seems essential to consider this kind of data only when other reference drugs are similarly evaluated, which permit ranking simultaneously classical NSAIDs and COX-2 selective inhibitors in terms of selectivity.

3.2. Docking studies

High-resolution X-ray structures of ovine COX-1 and murine COX-2 in complex with inhibitors lead to the 3D structure of the COX active site [31,32]. It is a long, narrow hydrophobic channel extending from the membrane-binding region to the protein core. Based on site-directed mutagenesis experiments and comparison of different crystal structures, the substitution of isoleucine 523 in COX-1 for a less bulky valine in COX-2 was proved to be the main contributing factor to the difference of the two binding sites (Fig. 3) [33]. This residue variation leads to a change in the size and shape of the two active sites (about 20% larger for COX-2 isoform) with an additional hydrophilic side-pocket characterizing COX-2. Such difference is often used to design COX-2 selective inhibitors [34]. Moreover, the substitution of histidine 513 in COX-1 for an arginine in COX-2, coupled with the latter, would also be responsible for the COX-2 selectivity of some inhibitors [35]. An imidazole ring at this position would not extent sufficiently in COX-1 for direct interactions with the sulfonamide group of most of reference COX-2 inhibitors [36].

As human COX-1 and -2 structures are not yet available in the PDB databank, these were first modeled by homology from the ovine COX-1 co-crystallized with flurbiprofen (1CQE) (with 91% identity) and from the murine COX-2 in complex with SC558 (6COX) (with 86% identity), respectively. The human/ovine COX-1 ($rmsd_{backbone}$ = 0.38 Å; $rmsd_{heavy}$ = 1.07 Å), human/murine COX-2 ($rmsd_{backbone}$ = 0.54Å; $rmsd_{heavy}$ = 1.10 Å) and also human/modeled ovine COX-2 ($rmsd_{backbone}$ = 0.60 Å; $rmsd_{heavy}$ = 1.20 Å) active sites are identical. The differences between isoforms are not located in the binding site but elsewhere. Here we are then assuming the binding mode of the compounds will be similar in both ovine and human isoforms. This hypothesis was tested and confirmed by docking studies of the studied compounds with the X-ray structure of ovine COX-1 and the modeled ovine COX-2 (data not shown). As the final goal consists of designing new anti-inflammatory drugs for humans, we describe here the docking studies in the human isoforms, assuming the COX-1/COX-2 selectivity is the same in both human and ovine species.

For the docking studies, input conformations of the five compounds were derived from X-ray studies [21,37–39] and took into account the form at physiological pH as reported in Fig. 2.

The compounds were docked in the human modeled isoforms using three different algorithms (Research, Gold and Autodock) with different scoring functions in order to highlight the solutions common to the three programs, supposed to be the most likely. These were then refined with the Discover3 module in order to account for amino acids flexibility of the active site (see Section 2). The other solutions can be, respectively, summarized as being unable to bind the active site while located at the protein surface, in bad agreement with the topology of the active site, or having an unusual conformation.

3.2.1. Binding modes of active compounds *1* and *2*

Two binding modes were identified in the **COX-2** isoenzyme for **1** (pink) and **2** (blue): the "lateral" (Fig. 4a) and the "inverse" modes (Fig. 4b). This result is in agreement with another study performed on **1** [40]. Both modes were identified in all three programs, only the refined solutions from the Gold program are given here.

In the lateral mode, the sulfonamide moiety fills the hydrophilic side-pocket and is involved in hydrogen bonds with such polar residues as His90 and Arg513. These interactions are essential for COX-2 inhibitory activity as exemplified by the binding interactions of SC558, an analogue of celecoxib, co-crystallized in the COX-2 active site [41]. The nitro group and the pyridinic nitrogen atom are close to the charged residue Arg120 lying at the entrance of the COX-2 active site. The phenoxy moiety fills the top of the channel and is stabi-

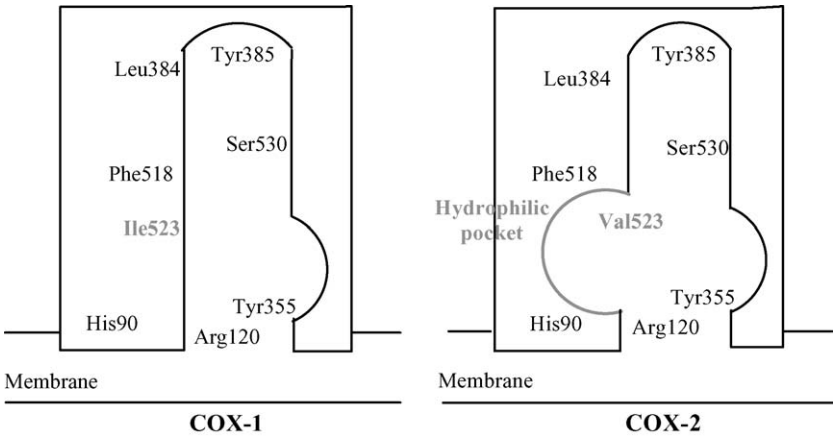

Fig. 3. Schematic representation of the active site of both isoenzymes COX-1 and COX-2.

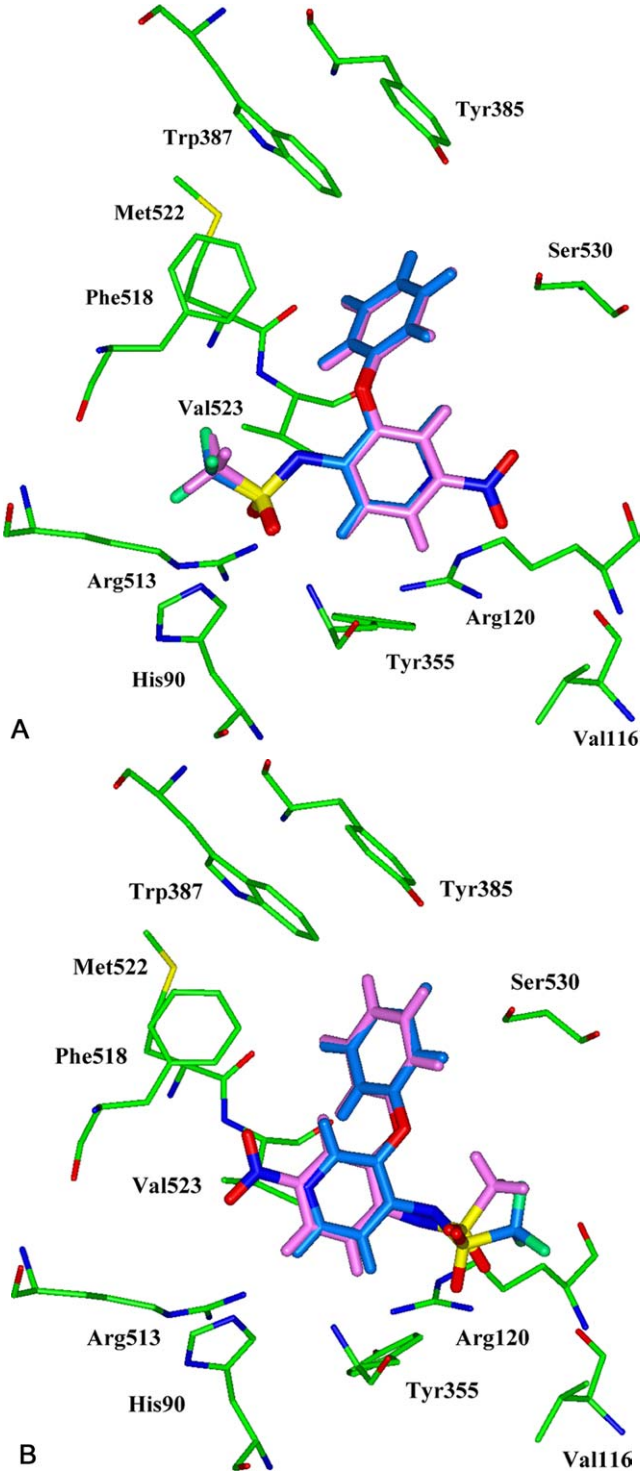

Fig. 4. a) "Lateral" binding mode; b) "Inverse" binding mode of **1** (pink) and **2** (blue) docked in the human COX-2 active site. Hydrogen's of amino acids are not depicted for clarity.

lized by different interactions, respectively, π–π interactions with Trp387 and Phe518 and CH–O bonds with Ser530 and Met522. CH–π interaction is also observed between Tyr355 and the phenyl or pyridine rings.

In the inverse mode, the sulfonamide group lies at the bottom of the channel and interacts with Arg120, while the nitro group and the pyridinic nitrogen atom are close to

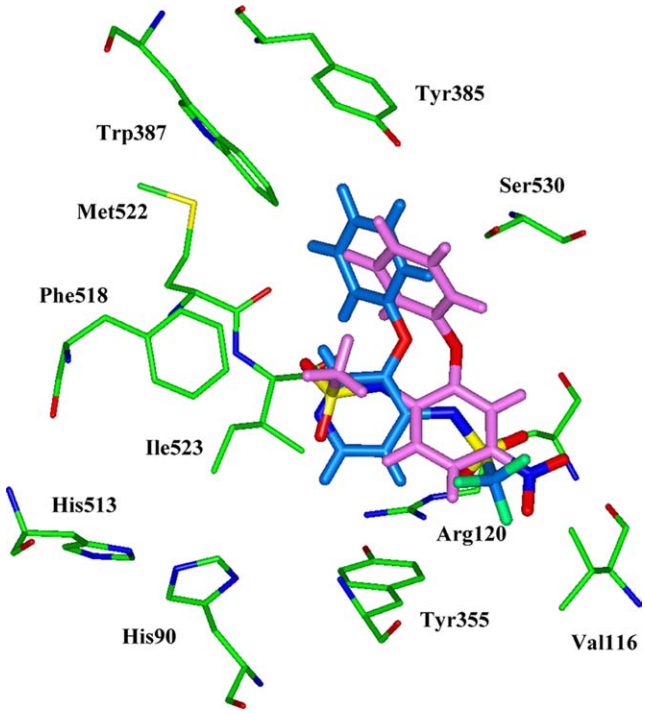

Fig. 5. Binding mode of **1** (pink) and **2** (blue) docked in the human COX-1 active site. Hydrogen's of amino acids are not depicted for clarity.

His90 and Arg513. The phenoxy group and central ring are involved in the same interactions as in the lateral mode.

Based on SAR studies and knowledge of the active site, it is difficult to preferentially select one of the two binding modes [40,42,43].

In order to understand the selectivity differences between **1** and **2**, docking studies were also performed in the modeled human **COX-1** isoform. Only one binding mode was obtained for the two compounds which remain in the hydrophobic channel (Fig. 5).

According to total interaction energy (ΔEtot), **1** seems to be more stable than **2** in COX-2 where it can accommodate the larger volume and interact favorably with polar amino acids of the hydrophilic side-pocket (Table 3). On the other hand, **2**, which is smaller than **1** (volume of 194.29 $Å^3$ against 206.50 $Å^3$ for **1**), is better positioned in COX-1 (ΔEtot = –34.23 kcal mol^{-1} for **2** and –26.46 kcal mol^{-1} for **1**) where H-bond interactions are observed with Arg120. Such analyses could explain the pharmacological profile of each compound: **1** and **2** preferentially inhibit COX-2 and COX-1 enzymes, respectively.

*3.2.2. Rationalization of the inactivity of compounds **3–5***

Analysis of inactive molecules is an important step to understand the essential features for a given activity. Therefore, **3–5** were also docked in the COX-2 active site and compared to the active compounds.

Compounds **3** and **4** adopt the lateral and inverse modes but with smaller total binding energy than **1** or **2** (Table 3). Indeed, an unfavorable interaction is observed between the protonated nitrogen of **3** and Arg513, His90, or Arg120. As a

Table 3
Interaction energies for compounds **1**–**5** in human COX-1 and/or COX-2 isoforms

Compound	Enzyme	Mode	ΔEcb [a]	ΔEvdw [a]	ΔEsolv [a]	ΔEtot [a]
1	*COX-2*	Lat	–21.30	–18.31	2.73	–36.88
		Inv	–17.46	–19.39	2.60	–34.25
	COX-1		–10.49	–18.03	2.06	–26.46
2	*COX-2*	Lat	–17.11	–17.60	2.69	–32.02
		Inv	–16.20	–17.87	2.51	–31.56
	COX-1		–17.85	–18.07	1.69	–34.23
3	*COX-2*	Lat	–13.03	–16.47	2.23	–27.27
		Inv	–16.52	–15.61	2.58	–29.55
4	*COX-2*	Lat	–9.64	–16.67	1.26	–25.05
		Inv	–6.67	–17.70	1.25	–23.12
5	*COX-2*	Inv	–7.19	–20.21	1.17	–26.23

Total interaction energy (ΔEtot) is composed of van der Waals (ΔEvdw) and Coulombic (ΔEcb) terms and of an electrostatic contribution of the solvation energy (ΔEsolv).

[a] All energies are expressed in kcal mol^{-1}.

result, a positive charge would not be suitable in the COX-2 active site and would be responsible for the inactivity of **3**. In the case of **4**, the protonated nitrogen of sulfonamide is involved in an intra-molecular H bonding interaction with the oxygen of the phenoxy group, forcing the compound in a restrained position. Such bond is also observed in the crystal structure of **4** [21]. Moreover, the weaker negative partial charge on the oxygen's of the sulfonamide moiety and the position of the pyridine nitrogen lead to weaker interactions with polar residues as His90, Arg513 and Arg120.

Because of its bulky volume, the *N*-methyl group of **5** is unable to access the hydrophilic pocket. Only the inverse mode is therefore observed. This additional CH_3 moiety leads to conformational restraints in the active site and some interactions are therefore reduced or lost. Indeed, π–π interactions with Trp387 and Phe518 are missing and the nitro group interacts weakly with His90 and Arg513.

3.2.3. Pharmacophore and interactions model in the COX-2 active site

Docking analyses of active and inactive compounds led us to suggest a COX-2 pharmacophore model with essential, or important, features for COX-2 activity and important interactions in the COX-2 active site for this family of inhibitors (Fig. 6). The distances between the molecular functions depicted in Fig. 6 were calculated from complexes of **1** and **2** in the COX-2 active site for the two binding modes and represent the smallest and largest values. A suitable position of the two polar groups near Arg120 and in the hydrophilic side-pocket seems to be important. Moreover, involvement of the phenyl ring in π–π interactions at the top of the channel probably leads to a better COX-2 activity.

3.3. Prediction of new compounds

Mainly because of its smaller volume (as seen in the docking studies), **2** preferentially inhibits the COX-1 isoform, unlike **1**. Therefore, in order to reverse its selectivity, we propose to take advantage of a structural difference between the two isoforms observed in the upper part of the channel to introduce new structural features. Indeed, a conserved amino acid, Leu384, is oriented differently in each isoenzyme due to the effects of a residue at position 503. In COX-1, Phe503 with its large size pushes Leu384 side chain into the top part of the channel. In COX-2, the smaller Leu503 allows Leu384 to orient away from the active site, generating a small lipophilic alcove (Fig. 7) [44]. This structural difference was taken into account to modify **2** and to try to reverse its selectivity. Such strategy has already been used to design COX-2 selective compounds [45]. The "leucine tickle region" is located close to the *para* position of the phenoxy group of **2** in both binding modes, leading to the design hypothesis that substitution of a small lipophilic group (X) would introduce COX-2 selectivity (Fig. 7).

3.3.1. Synthesis and pharmacological evaluation of new compounds

Compounds **6** and **7** were then synthesized and their COXs inhibitory potency was preliminarily tested by an in vitro enzyme assay. Compound **8** was also designed to confirm our hypothesis (Fig. 8 and Table 4).

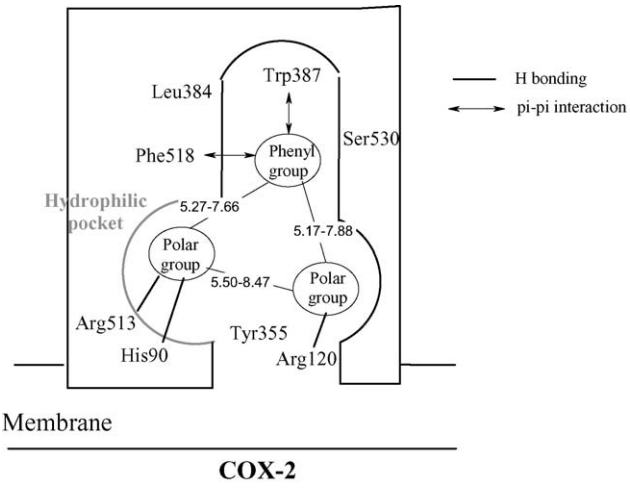

Fig. 6. COX-2 pharmacophore model inside a schematic COX-2 active site and important interactions between the pharmacophoric features and amino acids. Distances are expressed in angstrom.

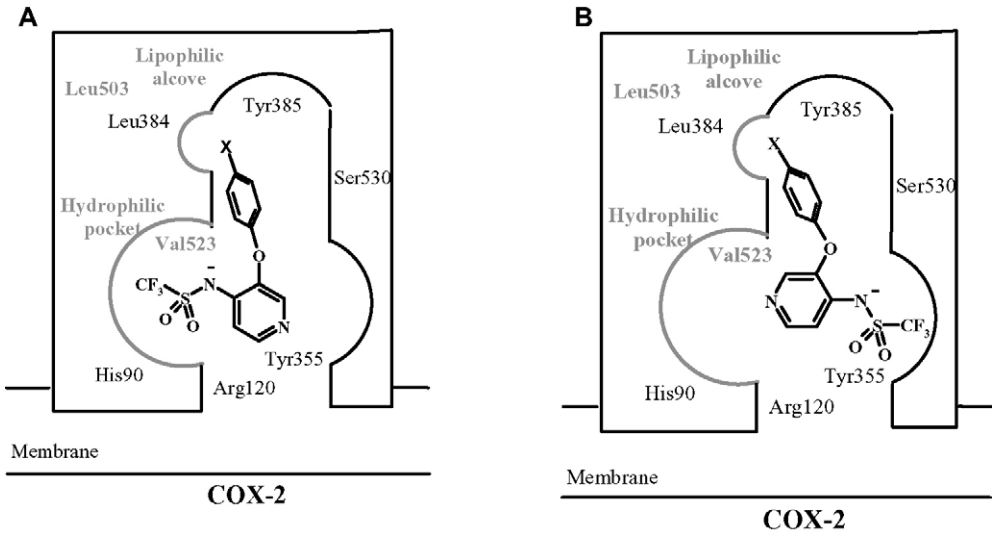

Fig. 7. Structure of proposed compounds, displaying a small lipophilic group (X) in *para* position of the phenoxy moiety, depicted in a schematic COX-2 active site, following a) the lateral mode and b) the inverse mode.

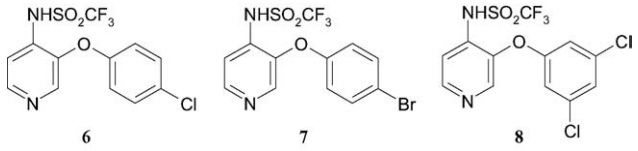

Fig. 8. Structure of compounds **6**–**8**.

Table 4
% Inhibition (or IC_{50}) of **2**, **6**–**8** on ovine assay **c** and human COX-2 assay **b**

Compound	% Inhibition ovine COX-1 (100 μM)*,c	% Inhibition ovine COX-2 (100 μM)*,c	IC_{50} human COX-2 (μM)*,b
2	15.53 ± 4.65	–8.59 ± 12.33**	> 100
6	76.66 ± 5.15	18.35 ± 8.05	48.8
7	–9.62 ± 15.90**	46.40 ± 0.78	20.7
8	Inactive	Inactive	> 100

* Details in experimental section. ** Inactive.
[b] Human assay **b**: enzyme–ligand incubation time of 5 min and arachidonic acid incubation time of 3 min.
[c] Ovine assay **c**: enzyme–ligand incubation time of 5 min and arachidonic acid incubation time of 2 min.

Compound **6** is characterized by a preferential COX-1 inhibition but shows a better COX-2 inhibitory activity than **2**. On the other hand, compound **7** is a selective COX-2 inhibitor with an improved COX-2 activity in comparison with compound **2**. Compound **8** is inactive for both isoforms.

Although compound **2** shows quite different activities in Tables 2 and 4, theses values are not comparable because they are issued from different kind of assays. This assumption was reported several times in literature [46].

3.3.2. Rationalization

As a result, unlike bromine, the chlorine substitution is not sufficient to obtain COX-2 selectivity and to fill the lipophilic alcove because of its small volume (22.14 $Å^3$ against 29.38 $Å^3$ for bromine). Therefore, compound **6** remains capable of binding COX-1 whereas compound **7** cannot. The bromine substitution is sufficient to reverse the selectivity.

Compound **8**, with two chlorine atoms in the *meta* positions of the phenyl group, does not show any activity for both isoforms. Docked complexes of **8** in COX-2 show that the chlorine atoms are not positioned in a good way to fill the lipophilic alcove in the lateral or the inverse mode (data not shown). Therefore, these first results confirm our hypothesis.

In addition, electronic distribution of a dichlorophenyl group compared to a chloro- or a bromophenyl one is quite different as shown by MEP profiles depicted in Fig. 9. Indeed, unlike dichlorophenyl, a more negative attractive MEP area is observed for bromo- and chlorophenyl moieties above the central ring. Such differences could partly explain the inactivity of **8** for both isoforms. Indeed, MEP profiles of aromatic compounds have already been correlated with binding affinities in the literature [47,48]. Although CH–π interactions seem to be important in the COX-2 binding (Fig. 6), the dichlorophenyl moiety would lead to bad contacts with aromatic residues in the top part of the channel.

3.3.3. New pharmacophore model in the COX-2 active site

From these analyses, our pharmacophore model in the COX-2 active site can be complemented by adding a small hydrophobic group positioned inside the lipophilic alcove (Fig. 10). This hypothesis is a first approach to explain COX-1/COX-2 inhibition and compound selectivity. It may be used to identify original lead compounds with COX-2 selective inhibition.

4. Conclusions

The pharmacological profile of pyridinic analogues of nimesulide was rationalized and compared to the parent compound by docking studies. Two binding modes, lateral and inverse, were observed where the sulfonamide group fills either the hydrophilic side-pocket or the bottom part of the

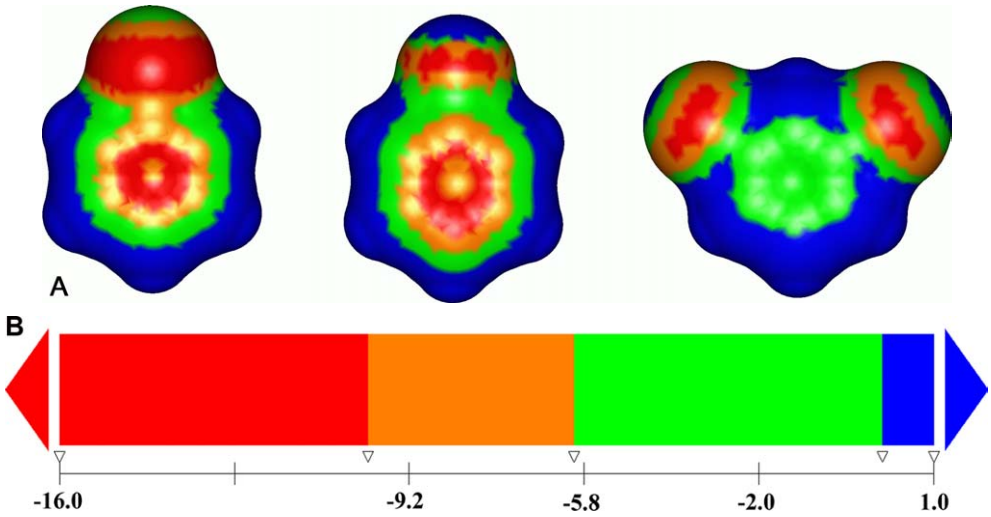

Fig. 9. MEP profile calculated for a) bromo-, b) chloro- and c) dichlorophenyl moieties and represented on the Connolly surface of each structure.

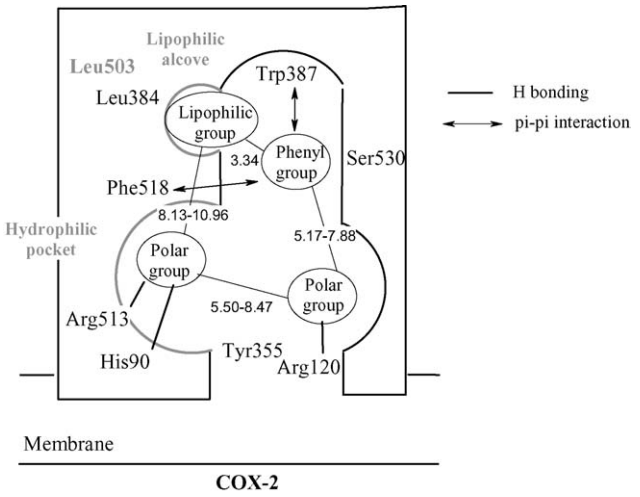

Fig. 10. Improved COX-2 pharmacophore and interactions model inside a schematic COX-2 active site. Distances are expressed in angstrom.

channel. In order to reverse the selectivity of **2**, preferentially inhibiting COX-1, structural modifications were proposed. From the knowledge of a small lipophilic alcove specific to COX-2, compound **7** was designed with a bromine substituent in the *para* position of phenoxy group. The latter compound proved to inhibit preferentially COX-2 while **2** did not. As a result, **7** can be considered as a new potential hit for COX-2 inhibition.

Acknowledgements

Catherine Michaux and Caroline Charlier acknowledge the FNRS for financial support. This work was also supported by a grant of the French Community of Belgium (no. 99/04–249).

References

[1] J.J. Dubost, M. Soubrier, B. Sauvezie, Rev. Med. Interne 20 (1999) 171–178.
[2] J.R. Vane, Nat. New Biol. 231 (1971) 232–235.
[3] D.A. Kujubu, B.S. Fletcher, B.C. Varnum, R.W. Lim, H.R. Herschman, J. Biol. Chem. 266 (1991) 12866–12872.
[4] L.J. Crofford, J. Rheumatol. 24 (Suppl. 49) (1997) 15–19.
[5] K. Seibert, Y. Zhang, K. Leahy, S. Hauser, J. Masferrer, W. Perkins, L. Lee, P. Isakson, Proc. Natl. Acad. Sci. USA 91 (1994) 12013–12017.
[6] B. Cryer, M.B. Kimmey, Am. J. Med. 105 (1998) 20S–30S.
[7] A. Whelton, Am. J. Med. 106 (1999) 13S–24S.
[8] N.S. Buttar, K.K. Wang, Mayo Clin. Proc. 75 (2000) 1027–1038.
[9] C. Michaux, C. Charlier, Mini-Reviews in Med, Chem. 4 (2004) 603–615.
[10] L. Parente, M. Perretti, Biochem. Pharmacol. 65 (2003) 153–159.
[11] C.A. Thompson, Am. J. Health. Syst. Pharm. 61 (2004) 2234–2236 (2238).
[12] S.S. Shaftel, J.A. Olschowka, S.D. Hurley, A.H. Moore, M.K. O'Banion, Brain Res. Mol. Brain Res. 119 (2003) 213–215.
[13] N.V. Chandrasekharan, H. Dai, K.L. Roos, N.K. Evanson, J. Tomsik, T.S. Elton, D.L. Simmons, Proc. Natl. Acad. Sci. USA 99 (2002) 13926–13931.
[14] J. Schwab, H.J. Schluesener, S. Laufer, Lancet 361 (2003) 981–982.
[15] K. Subbaramaiah, A.J. Dannenberg, Trends Pharmacol. Sci. 24 (2003) 96–102.
[16] Z.H. Feng, T.G. Wang, D.D. Li, P. Fung, B.C. Wilson, B. Liu, S.F. Ali, R. Langenbach, J.S. Hong, Neurosci. Lett. 329 (2002) 354–358.
[17] P.S. Aisen, K.A. Schafer, M. Grundman, E. Pfeiffer, M. Sano, K.L. Davis, M.R. Farlow, S. Jin, R.G. Thomas, L.J. Thal, JAMA 289 (2003) 2819–2826.
[18] I.A. Tavares, P.M. Bishai, A. Bennett, Arzneimittelforschung 45 (1995) 1093–1095.
[19] L. Cullen, L. Kelly, S.O. Connor, D.J. Fitzgerald, J. Pharmacol. Exp. Ther. 287 (1998) 578–582.
[20] J.P. Famaey, Inflamm. Res. 46 46 (1997) 437–446.
[21] F. Julémont, X. de Leval, C. Michaux, J. Damas, C. Charlier, F. Durant, B. Pirotte, J.M. Dogne, J. Med. Chem. 45 (2002) 5182–5185.
[22] F. Julémont, X. de Leval, C. Michaux, J.F. Renard, J.-Y. Winum, J.-L. Montero, J. Damas, J.-M. Dogné, B. Pirotte, J. Med. Chem. 47 (2004) 6749–6759.

[23] X. de Leval, J. Delarge, P. Devel, P. Neven, C. Michaux, B. Masereel, B. Pirotte, J.L. David, Y. Henrotin, J.-M. Dogné, Prost. Leukot. Essent. Fatty Acids 64 (2001) 211–216.
[24] Biosym/MSI, InsightII 97.0: HOMOLOGY, Molecular Simulations Inc., San Diego, 1997.
[25] T.N. Hart, S.R. Ness, Dockvision; Version 1.0.3, ed., Alberta, 1998.
[26] G. Jones, P. Willett, R.C. Glen, A.R. Leach, R. Taylor, Gold; Version 1.2, ed., Astex Technology, Cambridge, UK, 2001.
[27] G.M. Morris, D.S. Goodsell, R.S. Halliday, R. Huey, W.E. Hart, R.K. Belew, A.J. Olson, J. Comput. Chem. 19 (1998) 1639–1662.
[28] Accelrys, Discover3; Version 2.98, ed., Accelrys Inc., San Diego, 1998.
[29] B. Honig, K.A. Sharp, A.-S. Yang, J. Phys. Chem. 97 (1993) 1101–1109.
[30] M.J. Frisch, G.W. Trucks, H.B. Schlegel, Gaussian 98; Revision A.11, ed., Gaussian, Inc., Pittsburgh PA, 2001.
[31] D. Picot, P.J. Loll, R.M. Garavito, Nature 367 (1994) 243–249.
[32] C. Luong, A. Miller, J. Barnett, J. Chow, C. Ramesha, M.F. Browner, Nat. Struct. Biol. 3 (1996) 927–933.
[33] J.K. Gierse, J.J. McDonald, S.D. Hauser, S.H. Rangwala, C.M. Koboldt, K. Seibert, J. Biol. Chem. 271 (1996) 15810–15814.
[34] A. Palomer, J. Pascual, M. Cabré, L. Borràs, G. Gonzàlez, M. Aparici, A. Carabaza, F. Cabré, M.L. Garcia, D. Mauleón, Bioorg. Med. Chem. Lett. 12 (2002) 533–537.
[35] E. Wong, C. Bayly, H.L. Waterman, D. Riendeau, J.A. Mancini, J. Biol. Chem. 272 (1997) 9280–9286.
[36] R.G. Kurumbail, A.M. Stevens, J.K. Gierse, J.J. McDonald, R.A. Stegeman, J.Y. Pak, D. Gildehaus, J.M. Miyashiro, T.D. Penning, K. Seibert, P.C. Isakson, W.C. Stallings, Nature 384 (1996) 644–648.
[37] L. Dupont, B. Masereel, P. de Tullio, B. Pirotte, J. Delarge, Acta Crystallogr. C51 (1995) 507–509.
[38] C. Michaux, C. Charlier, F. Julémont, J.-M. Dogné, X. de Leval, B. Norberg, B. Pirotte, F. Durant, Acta Crystallogr. C58 (2002) o88–o89.
[39] C. Michaux, C. Charlier, F. Julémont, B. Norberg, J.-M. Dogné, F. Durant, Acta Crystallogr. E57 (2001) 1012–1013.
[40] R. Garcia-Nieto, C. Perez, F. Gago, J. Comput. Aided Mol. Des. 14 (2000) 147–160.
[41] R.G. Kurumbail, A.M. Stevens, J.K. Gierse, J.J. McDonald, R.A. Stegeman, J.Y. Pak, D. Gildehaus, J.M. Miyashiro, T.D. Penning, K. Seibert, P.C. Isakson, W.C. Stallings, Nature 384 (1996) 644–648.
[42] C. Marot, P. Chavatte, D. Lesieur, Quant. Struct.-, Act. Relat. 19 (2000) 127–134.
[43] R. Pouplana, J.J. Lozano, J. Ruiz, J. Mol. Graph. Model. 20 (2002) 329–343.
[44] C.I. Bayly, W.C. Black, S. Léger, N. Ouimet, M. Ouellet, M.D. Percival, Bioorg. Med. Chem. Lett. 9 (1999) 307–312.
[45] A.S. Kalgutkar, B.C. Crews, S.W. Rowlinson, A.B. Marnett, K.R. Kozak, R.P. Remmel, L.J. Marnett, Proc. Natl. Acad. Sci. USA 97 (2000) 925–930.
[46] J.K. Gierse, C.M. Koboldt, M.C. Walker, K. Seibert, P.C. Isakson, Biochem. J. 339 (1999) 607–614.
[47] V. Prasad, E.T. Birzin, C.T. McVaugh, R.D. Van Rijn, S.P. Rohrer, G. Chicchi, D.J. Underwood, E.R. Thornton, A.B. Smith, R. Hirschmann, J. Med. Chem. 46 (2003) 1858–1869.
[48] S. Mecozzi, A.P. West, D.A. Dougherty, Proc. Natl. Acad. Sci. USA 93 (1996) 10566–10571.